Charge distribution on the water/γ-Fe 2 O 3 interface

N. Ntallis, V. Peyre, R. Perzynski, E. Dubois, K.N. N Trohidou

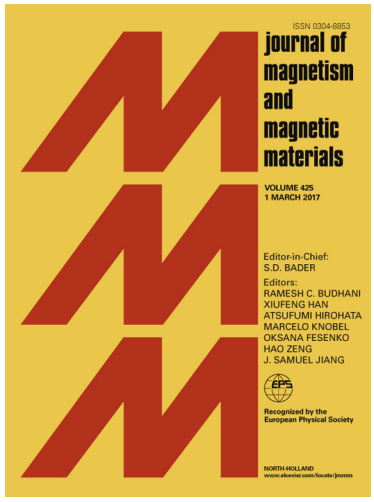

Charge distribution on the water/γ-Fe_2O_3 interface

N. Ntallis, V. Peyre, R. Perzynski, E. Dubois, K.N. Trohidou

PII: S0304-8853(18)32744-6
DOI: https://doi.org/10.1016/j.jmmm.2019.03.132
Reference: MAGMA 65147

To appear in: *Journal of Magnetism and Magnetic Materials*

Received Date: 30 August 2018
Revised Date: 26 February 2019
Accepted Date: 31 March 2019

Please cite this article as: N. Ntallis, V. Peyre, R. Perzynski, E. Dubois, K.N. Trohidou, Charge distribution on the water/γ-Fe_2O_3 interface, *Journal of Magnetism and Magnetic Materials* (2019), doi: https://doi.org/10.1016/j.jmmm.2019.03.132

Manuscript Template (A4 size)

Charge distribution on the water/γ-Fe_2O_3 interface

N. Ntallis[1]. V. Peyre[2]; R. Perzynski [2]; E. Dubois,[2], K. N. Trohidou[1]

[1] NCSR Demokritos, Institute of Nanoscience and Nanotechnology, Agia Paraskevi, Greece

[2]Sorbonne Univ, CNRS, UPMC Univ Paris 06, Lab PHENIX, Case 51,4 Pl Jussieu, F-75005 Paris, France

[*]Corresponding author e-mail: k.trohidou@inn.demokritos.gr, Phone: +30 (0) 6503395, Fax: +30 (0) 6519430

Abstract

We have studied the charge distribution in the γ-Fe_2O_3 interface with H_2O, for two different structures (films and spherical nanoparticles) with Density functional (DFT) molecular dynamics calculations. Our results show that the adsorption energy depends on the shape of the surface and in the case of the films also on the orientation of the crystal and that the ionic state of iron atoms increases with the addition of water in both structures while the magnetic moments of the structures do not show any significant change. The mean displacement of the charge with temperature is significant only in the spherical nanoparticles. The average electrostatic potential decreases with the addition of water and shows an oscillatory behavior near the surface.
.

Keywords: DFT; γ-Fe_2O_3 nanoparticles; charge distribution; water molecules

1. Introduction

Interfaces between transition metal oxides and liquid water have attracted considerable attention due to their importance in atmospheric science [1], catalysis [2], energy storage [3], colloid chemistry [4] and energy harvesting [5,6]. It is known that most metal oxide surfaces react with water and are partially covered with molecular H_2O and/or hydroxyl species [7, 8] which can significantly affect the surface reactions, thus affecting their functionality in various applications.

Iron oxides are among the most important environmental sorbents and play important role in the composition and quality of natural water. Hematite (α-Fe_2O_3) is a very stable material and often the end form of transformations of other iron oxides. Hematite-water interactions have been extensively studied experimentally for nanoparticle and film structures [9-11]. Moreover for film structures hematite/water interfaces have been also studied by means of Density Functional Theory (DFT) calculations [12-15]. In these studies, it has been demonstrated that the presence of water affects the charge distribution of the oxide surface.

In contrast, γ-Fe_2O_3/water interfaces have been much less studied. Maghemite exhibits ferrimagnetic ordering with a net magnetic moment (2.5 μ_B per formula unit) and high Néel temperature (~950 K), which together with its chemical stability and the low cost leads to a wide range of applications in recording media [16] and in biomedicine, as they are biocompatible and potentially non-toxic to humans

[17,18]. Recently, there is an increasing interest in maghemite nanoparticles for thermoelectric applications. It has been shown that when they are dispersed in ionic liquids they increase the thermoelectric efficiency of these liquids [19, 20]. A critical factor for the successful synthesis of ionic liquid based ferrofluids (FF) is the colloidal stability of the nanoparticles. Therefore the study of the charge distribution on the surface of the nanoparticles is of great importance.

From the charge distribution we can evaluate the mean electrostatic potential in the presence of water inside and up to a distance from the surface for these structures. In this way we can define the zeta (ζ) potential [21] which is the electrostatic potential just outside the surface of the structure. This quantity can give an estimation of the degree of electrostatic repulsion between adjacent charged structures. In particular its calculation is of great importance for evaluation of the colloidal stability of nanoparticles in FF, since it is a measure of the electrostatic repulsion charged particles in dispersion.

In the present work the charge distribution of the γ-Fe_2O_3/water in semi-infinite (film) structures and spherical nanoparticles is studied by means of molecular dynamics density functional theory calculations. In what follows we first present the methodology, and we continue with the results and discussion of the adsorption energy. Next, the charge distribution and the effect of the charge displacement for a finite temperature are discussed. The electrostatic potential for the studied structures follows together with an estimation of the zeta potential. Finally our concluding remarks are presented.

2. Methodology

We employ DFT spin-polarized density functional theory via the Vienna Ab Initio Simulation Package (VASP) [22-24] for (semi-infinite) film and (finite) nanoparticle structures We have studied two films with two different crystal orientations, the 100 (100 film) and the 001 (001 film). The finite structure is a spherical nanoparticle. The geometries are optimized with a tolerance of 10^{-4} eV for the electronic relaxation and 10^{-3} eV for the ionic relaxation.

The exchange correlation functional chosen is the one proposed by Perdew-Burke-Ernzerhof (PBE). Van der Waals corrections have been included in the calculations, by using the D2 method of Grimme [25]. The interactions between the electrons and ions were described using the projector-augmented-wave (PAW) method. A cutoff of 550eV was used for the plane wave expansion in all cases. The GGA+U approach was used to treat localized states as proposed by Duradev et al. in ref [26]. The tuning of the effective exchange parameter $U_{eff} = U - J$ was extracted from the bulk calculations. A value of $U_{eff} = 4.2eV$ predicts the cell dimensions of a=b=8.33 Å and c= 25.11 Å.

Our initial structures were formed from the structure of the bulk unit cell [27]. The film systems consist of 7 layers of atoms with the two bottom layers fixed. For the film systems the initial cells have dimension of 25.0 and 8.33 Å in the film's plane and 25 Å normal to this plane. From the 25 Å at least 16 Å are considered to be empty space in order to break periodicity along this direction. The nanoparticle of diameter ~ 1.7nm is constructed from replication of the bulk unit cell followed by a trimming process that produces the spherical shape. For the nanoparticle in order to break periodicity along all directions a computational cell of 33 x 33x 33 Å has been used. For the film systems a 1x7x5 and 5x7x1 Monkhorst Pack grid was used and for the particle only the gamma point is taken. On the surface of the film systems up to 4 water molecules were placed and up to 5 on the surface of the spherical nanoparticle. For the cells used in the calculations the one water molecule refers to coverage of 2.5% for the film systems and 1% for the spherical nanoparticle. Before relaxing the maghemite/ structures with the addition of water, the maghemite structures without water were relaxed using the same convergence criteria in both cases.

For the calculation of the charge distribution on the γ-Fe_2O_3/water interfaces for the three structures, we employ DFT molecular dynamics calculations at constant temperature using the Nosé-thermostat in the

VASP package. The calculations were performed at temperature T=0 K and T=300K. The time step used for the integration was 1fs and averages were taken every 1000 steps.

3 Results and discussion

3.1 Structural properties

Figures 1a, 1b and 1c show the relaxed structures, after the addition of the maximum number of water molecules i.e. 4 for the two films and 5 for the nanoparticle. Our calculations show that the addition of water above the Fe ions leads to energetically favored coordination of water with the OH bond axis parallel to the local Fe environment and the addition above the O atoms of the oxide leads to energetically favored coordination of water with the OH bond axis pointing almost normal to the local environment.

We find the mean distance between water molecules and γ-Fe_2O_3 2.19 Å for the 100 film and 2.07 Å for the 001 film, since the different coordination of the surface planes affects the equilibrium distance. In the spherical nanoparticle the distance between water and γ-Fe_2O_3 is found smaller, 1.94 Å. In all cases water sustains its molecular structure.

In order to study the effect of the water on the interatomic distance variation in Figure 2 we have plotted the radial distribution function (rdf) as function of the radial distance for the three structures, before (red lines) and after (blue lines) the addition of water. The rdf curves with water have been calculated for the largest number of water molecules added, i.e. 4 for the films and 5 for the spherical particle. For the film systems (figs 2(a) and 2(b)) an increase of the Fe-O bond length is found after the addition of water arising from the surface atoms as the whole curve is shifted to the right. The mean relative difference of the Fe-O bond is 3.4% and 4.1% for the 100 and 001 cases respectively. In the nanoparticle (fig 2c) the curve is shifted to the left, thus the Fe-O distance decreases with respect to the case without water. In this case the mean relative difference of the Fe-O bond is 4.9%. This means that in the nanoparticle the presence of water allows further relaxation of the surface atoms. The difference with the film structures can be attributed to the smaller coordination number of the surface atoms in the nanoparticle.

3.2 Adsorption energy

Next we calculate the adsorption energy for the three structures which is defined as

$$E_{ads} = E(maghemite + water) - E(maghemite\_no\_water) - N * E(water\_molecule). \quad (1)$$

Here $E(maghemite + water)$ is the energy of the full structure, $E(maghemite\_no\_water)$ is the energy of the maghemite structure without water, N is the number of water molecules and $E(water\_molecule)$ is the energy of the isolated water molecule.

Figures 3(a), 3(b) and 3(c) show the adsorption energy for these three structures as a function of the number of water molecules added. From figures 3(a) and 3(b), we can see that in the films the adsorption is energetically more favorable in the 001 film. In the spherical nanoparticle the adsorption energy has larger values, indicating that the finite structure is more sensitive in the addition of water as it has also been observed in adsorption energy values of spherical hematite nanoparticles. As it has been demonstrated in refs [28, 29] the size of the particle plays an important role in the adsorption energy for metallic and oxide systems as larger adsorption energies have been found for small particle sizes in comparison to film structures. For very small particles the most of the Fe atoms are on the surface and they have smaller number of O neighboring atoms than a perfect film plane. These sites interact better with water as it has been demonstrated for Mg atoms [30]. This is consistent with the rdf calculations of section 3.1 and it is attributed as we show above, to a relaxation of a larger number of atoms on the surface of the nanoparticle.

We must note that adsorption energy in the films and the nanoparticle cannot be directly compared as though the coverage of water is close in the two cases, because of different number of surface sites. For this reason in Fig. 3(d) we have plotted the adsorption energy per atom for the three maghemite structures. Initially the energy difference of the nanoparticle and the 001 film structure is very small and increases as more water molecules are added. From figure 3(d) we see that the slope of the $E_{ads}/atom$ is larger for the nanoparticle. This indicates the ability of the nanoparticle to adsorb more water molecules before saturation.

3.3 Charge distribution

In order to study the charge distribution of these three structures the Bader charge analysis which is based on Gauss's law, has been used. In this analysis, the definition of an atom is based purely on the electronic charge density, since it uses the so called zero flux surface, in which the charge density has a minimum perpendicular to the surface [31]. The charge density is expected to have a minimum between atoms making consequently this surface a natural choice to separate atoms, starting from the charge density distribution.

Figures 4 (a and b), 5(a and b) and 6(a and b), show the charge of the Fe(a) and O(b) atoms as a function of the atom number for the 100 film, the 001 film and the nanoparticle respectively, before and after the addition of water at temperature T=0K. This charge (in units of electron) is given as

$$q = q_{valence} - q_{bader} \quad (2)$$

where $q_{valence}$ is the valence charge calculated from the charge analysis and q_{bader} is the valence charge used in the DFT calculation (8 for Fe, 6 for O and 1 for H atoms). In these figures, the atoms are shorted in such a way that first the inner atoms are shown and they are followed by the surface atoms for each type of atom. The charge q, in all figures, is calculated for the largest coverage. As we can see from figs. 4a, 5a, 6a the charge distribution is mostly affected close to the surface of the structures. This effect is more pronounced for the nanoparticle system. We must note here that very little variation of the charge is found with the change of the temperature from 0 K to 300 K.

Tables 1-3 show indicatively the charges that have been found for some water bonded Fe atoms and for O and H atoms from the water molecules (denoted as O_w, H_w) before and after the addition of water on the surface of the γ-Fe_2O_3 structures. The charges of O_w and H_w before being added to the structure, were calculated using the Bader charge analysis for a single water molecule and were found equal to -1.31e and 0.65e respectively.

From these tables we can see a little increase of the water molecule charge, indicating a charge transfer from water molecules to the Fe bonded atoms of maghemite. The Fe atoms show an increase in their ionic state with the addition of water as their positive charge is increased. This can be attributed to the change of the Fe-O bond length with the presence of water (figs 2(a)-(c)). These variations of the charge indicate an ionic-covalent character of the bond between Fe and water.

Together with the charge we have calculated the spatial displacement of the charge centers (figures 4c, 5c, 6c) from the position coordinates of the associated atom to which the charge has been assign for the temperatures T=0K and T=300K. All graphs give the charge distribution as a function of the atom number for the largest number of water molecules, i.e. 4 for the film systems and 5 for the spherical particle. In these figures Fe and O atoms are shown in a single graph with Fe atoms first followed by O atoms. As we can see from figs. 4(b) and 5(b) in the films the mean displacement from the center of charges is very little affected from the temperature up to T=300K.
In the spherical particle (fig. 6(b)) there is an increase of the mean displacement as the temperature increases. This clearly indicates that the particle is more sensitive to thermal excitations. This is expected, because the nanoparticle has smaller coordination number and broken bonds on the surface. As the mean charge displacement is evident the charge distribution may vary spatially as the

temperature increases expanding the interaction range of the nanoparticle for a wide range of temperatures. This is important for the γ-Fe_2O_3 nanoparticles use in ferrofluids for thermoelectric applications, since the temperature dependence of the charge displacement will influence their colloidal stability.

3.4 Average electrostatic potential

Figure 7 shows the average electrostatic potential as a function of the distance from the surface of the maghemite structures. In figures 7a and 7b the electrostatic potential has been plotted from the distance 8 Å just above the film surface (starting from the bottom layer) and for larger distances and in the nanoparticle case (fig 7c) from the distance 8 Å from the center of the particle (the particle radius being ~8.5 Å). The green lines show the systems with no water in all cases, the red lines with two and the blue lines with four water molecules respectively in the two films. For the spherical particle only the case of five water molecules is shown (fig 7c), since our calculation showed that the cases with smaller number of water molecules do not show a significant variation from the case without water in the average electrostatic potential. As it can be seen from figures 7, the films have larger electrostatic potential as they are periodic in x-y plane. Moreover in all cases as water is added to the structure the potential reduces. In the film systems this reduction is larger from that in the nanoparticle, as the percentage of the coverage of water is larger. For the spherical particle the reduction of the potential with the addition of water is small but measurable. In the three graphs the marked regions near the surface, show the oscillatory behavior of the potential, as it has been also observed in ref [8] for film metallic oxide structures. We must note that in this region above the surface of the structures we have an estimation of the ζ (zeta) potential. The ζ potential decreases as more water molecules are added in the films. In the 001 film, with the addition of four water molecules the ζ potential reduces and changes sign. This can be attributed to the fact that, as it is shown in fig. 3, the 001 direction has the bigger adsorption energy; therefore it adsorbs water more easily. For the spherical particle the difference in the zeta potential is small between the water and without water case, and it can be attributed to the fact that due to its finite size the surface area is big part of the nanoparticle (~50%), consequently only a small number of active sites are covered with respect to the film systems, where along the x-y plane periodic conditions are applied. Therefore we expect that in this case by adding more water molecules on the surface of the nanoparticle we will enhance the average electrostatic potential. Some reduction of the surface potential has been also observed in hematite [32] and SiO surfaces [33] with the addition of excess charge on the surface.

3.5 Magnetic Properties.

In all structures a ferrimagnetic ordering has been used as initial spin structure. More specifically ferromagnetic ordering in tetrahedral sites, ferromagnetic ordering between octahedral sites and antiferromagnetic ordering between tetrahedral and octahedral sites is considered. In all cases studied the magnetic moment of the Fe atoms is found between 3.8-4.2 μ_B indicating that all Fe atoms are close +3 oxidation state. Table 4 shows the net magnetic moment M divided by the number of Fe atoms in the whole structure, before and after the addition of water. As we saw in section 3.1 the presence of water affects the Fe-O distances of the surface atoms and results to a small reduction of the magnetic moment of the bonded Fe atoms. So we have a small overall reduction of the net magnetic moment per atom as shown in table 4.

Conclusions

We have performed DFT molecular dynamics calculations to study the charge distribution and the electric field on interfaces between maghemite and water molecules for semi-infinite (film) and finite

(nanoparticles) structures. Our results show that the adsorption energy depends on the shape of the surface and in the case of the films also on the orientation of the crystal and that the ionic state of iron atoms increases with the addition of water in both structures. The mean displacement of the charge with temperature is significant in the spherical nanoparticles and makes them attractive for thermoelectric applications using ionic liquid based ferrofluids. The average electrostatic potential shows an oscillatory behavior close to the interface as it has also been observed in ref [8] that can be attributed to the rearrangement of charges when the water comes close to the surface of the particle. The average electrostatic potential is affected by the number of molecules (different amount of charge) added to the surface and by the shape of the structure in agreement with the finding of refs [34, 35].

Acknowledgements

This work was supported by the European Union's Horizon 2020 Research and Innovation Programme: under grant agreement No. 731976 (MAGENTA).
KNT and NN acknowledge the computational time granted from the Greek Research & Technology Network (GRNET) in the Greek National HPC facility ARIS (http://hpc.grnet.gr) under project NASIFMAG (pr004027).

References

[1] A.R. Ravishankara, Y Rudic, D.J. Wuebbles, Chem. Rev., 115 (2015) 3682

[2] H. Kuhlenbeck, S. Shaikhutdinov, H. J.Freund, Chem. Rev., 113 (2015) 3986

[3] M.V. Reddy, G.V. Subba Rao, B.V.R Chowdari, Chem.Rev., 113 (2013) 5364

[4] A. Philippe, G.E. Schaumann, Environ. Sci. Technol. 48 (2014) 8946

[5] K. Sivula, F. Le Formal, M. Grätzel, Chem. Sus. Chem., 4 (2012) 432

[6] J. Lützenkirchen, F. Heberling, F. Supljika, T. Preocanin, N. Kallay, F. Johann, L. Weisser P.J. Eng, Faraday Discuss., 180 (2015) 55

[7] M. Rentao, Z. Zhi-jian, D.I. Zdenek, G. Jinlong, Chem. Soc. Rev., 46 (2017) 1785.

[8] L. Vlcek et. al., Langmuir 23 (2007), 4925.

[9] L. Mazeina, A. Navrotsky, Chem. Mater., 19 (2007) 825.

[10] P. Liu, T. Kendelewicz, G. Brown, Jr., E. Nelson, S. Chambers, Surf. Sci., 417 (1998) 53.

[11] S. Yamamoto, T. Kendelewicz, J. Newberg, G. Ketteler, D. Starr, E. Mysak, K. Andersson, H. Ogasawara, H. Bluhm, M. Salmeron, G. Brown and A. Nilsson, J. Phys. Chem., 114 (2010) 2256.

[12] R. B. Wang, A. Hellman, J. Chem. Phys, 148 (2018) 094705

[13] G. F. von Rudorff, R. Jakobsen, K. M. Rosso, J. Blumberger, J. Phys.: Condens. Matter, 28 (2016) 394001

[14] Shuxia Yin , D.E. Ellis, Sur. Science, 602 (2008) 2047.

[15] R. Ovcharenko, E.Voloshina, J. Sauer, Phys. Chem. Chem. Phys., 18 (2016) 25560.

[16] R. Dronskowski, Adv. Funct. Mater., 11 (2001) 27.

[17] Q.A Pankhurst, J. Connolly , S.K. Jones, J. Dobson, J. Phys. D.-Appl. Phys. 36 (2003) R167.

[18] M. Levy, C. Wilhelm, J.M. Siaugue, O. Horner, J.C. Bacri, F.J. Gazeau, J. Phys. - Condens. Mat. 20 (2008) 204133.

[19] T. J. Salez, B. Huang, M. Rietjens, M. Bonetti, C. Wiertel-Gasquet, M. Roger, C. L. Filomeno, E. Dubois, R. Perzynski, and S. Nakamae, Phys. Chem. Chem. Phys., 19 (2017) 9409.

[20] M. Mamusa, J. Siriex-Plénet, F. Cousin, E. Dubois,V. Peyre, Soft Matter, 10 (2014) 1097.

[21] A. V. Delgado, F. Gonzalez-Caballero, R. J. Hunter, L. K. Koopal, J. Lyklema, Pure Appl. Chem., 77 (2005) 1753

[22] G. Kresse, J. Furthmuller, Comput. Mat. Sci., 6 (1996) 15

[23] G. Kresse, J. Furthmuller, Phys. Rev. B, 54 (1996) 11169

[24] E.R. Hernández, A. Rodriguez-Prieto,A. Bergara, D Alfè, Phys. Rev. Lett., 104 (2010) 185701.

[25] S.Grimme., J. Comp. Chem., 27 (2006) 1787

[26] S. L. Dudarev, G. A. Botton, S. Y. Savrasov, C. J. Humphreys, A. P. Sutton, Phys. Rev. B, 57 (1998) 1505

[27] T.J. Bastow, A. Trinchi, M.R. Hill, R. Harris, T.H. Muster, J. Magn. Matter., 321 (2009) 2677.

[28] I.V. Yudanov, M. Metzner, A. Genest,; N. Rosch, J. Phys. Chem. C, 112 (2008) 20269.

[29] M. Fernández-García, A. Martínez-Arias, J.C. Hanson, J.A. Rodríguez, Chem. Rev., 104 (2004), 4063.

[30] G. Pacchioni, Surf. Rev. Lett., 7 (2000), 2777

[31] G. Henkelman, A. Arnaldsson, and H. Jónsson, Comput. Mater. Sci., 36 (2006) 354.

[32] J. Lützenkirchen, T. Preočanin, F. Stipić, F. Heberling J. Rosenqvist, N. Kallay, Geo. et Cosmo. Acta 120 (2013) 479.

[33] B.M. Lowe, C.-K. Skylaris, N.G. Green , Y. Shibuta, T. Sakata, Japanese J. App. Phys. 57, ((2018) 04FM02

[34] G. Feng, R. Qiao, J. Huang, S. Dai ,BG. Sumpter, V. Meunier, Phys. Chem. Chem. Phys, 13 (2011) 1152.

[35] Y. Qiu, J. Ma, Y. Chen, Langmuir, 32, (2016) 4806

[36] K. Momma , F. Izumi, J. Appl. Crystallogr., 44 (2011), 1272

Figure captions

Figure 1. Relaxed structures after the addition of water molecules on the maghemite surface for a) the film along the 100 direction (100 film) b) the film along the 001 direction (001 film) and c) the spherical nanoparticle. All structures include the maximum number of water molecules (i.e. 4 for the films and 5 for the nanoparticle). Yellow balls represent Iron, red balls oxygen and white balls hydrogen atoms. Drawings have been made with VESTA software [36].

Figure 2. radial distribution function (rdf) as a function of the radial distance (r(Å)) for (a) the 100 film, (b) the 001 film and (c) the spherical nanoparticle.

Figure 3. Adsorption energy as a function of the water molecules added for (a) the 100 film, (b) the 001film and (c) the spherical nanoparticle and (d) the adsorption energy per atom (in γ-Fe_2O_3) as a function of the number of water molecules for the three structures.

Figure 4. The 100 film: Charge distribution of (a) Fe atoms and (b) O atoms before and after the addition of four water molecules. The numbering of x-axis starts from the inner atoms and continues with the surface atoms. (c) Spatial charge displacement from the associated atom, for two temperatures.

Figure 5. The 001 film: Charge distribution of (a) Fe atoms and (b) O atoms before and after the addition of four water molecules. The numbering of x-axis starts from the inner atoms and continues with the surface atoms. (c) Spatial charge displacement from the associated atom, for two temperatures.

Figure 6. The nanoparticle: Charge distribution of (a) Fe atoms and (b) O atoms before and after the addition of five water molecules. The numbering of x-axis starts from the inner atoms of the nanoparticle and continues with the surface atoms. (c) Spatial charge displacement from the associated atom, for two temperatures.

Figure 7. The average electrostatic potential as a function of the distance starting from the surface of the structures: for (a) the 100 film, (b) the 001 film and c) the spherical nanoparticle. Green lines show the system without water, red with two molecules of water and blue 4 water molecules. In the spherical nanoparticle the blue line shows 5 water molecules.

Table captions

Table 1. Indicative charge maxima of the Fe and water molecules for the 100 film before and after the addition of water.

Table 2. Indicative charge maxima of the Fe and water molecules for the 100 film before and after the addition of water.

Table 3. Indicative charge maxima of the Fe and water molecules for the spherical nanoparticle before and after the addition of water.

Table 4. Net magnetic moment per Fe atom for the three structures before and after the addition of water. The values are for largest water coverage, i.e 4 water molecules for the film structures and 5 water molecules for the nanoparticle.

Figures

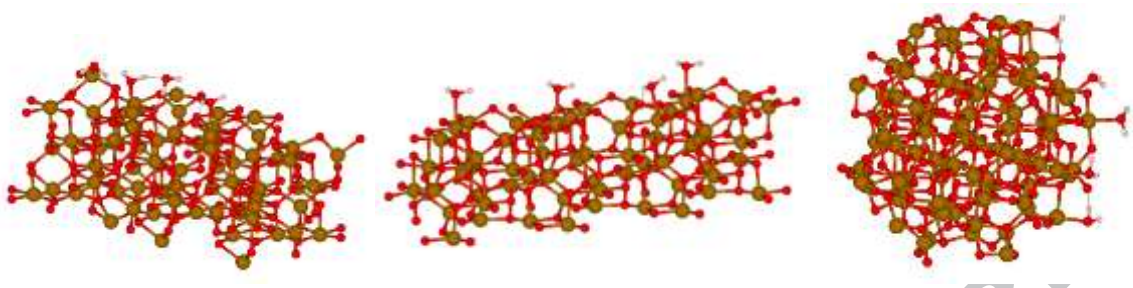

a) b) c)

Figure 1.

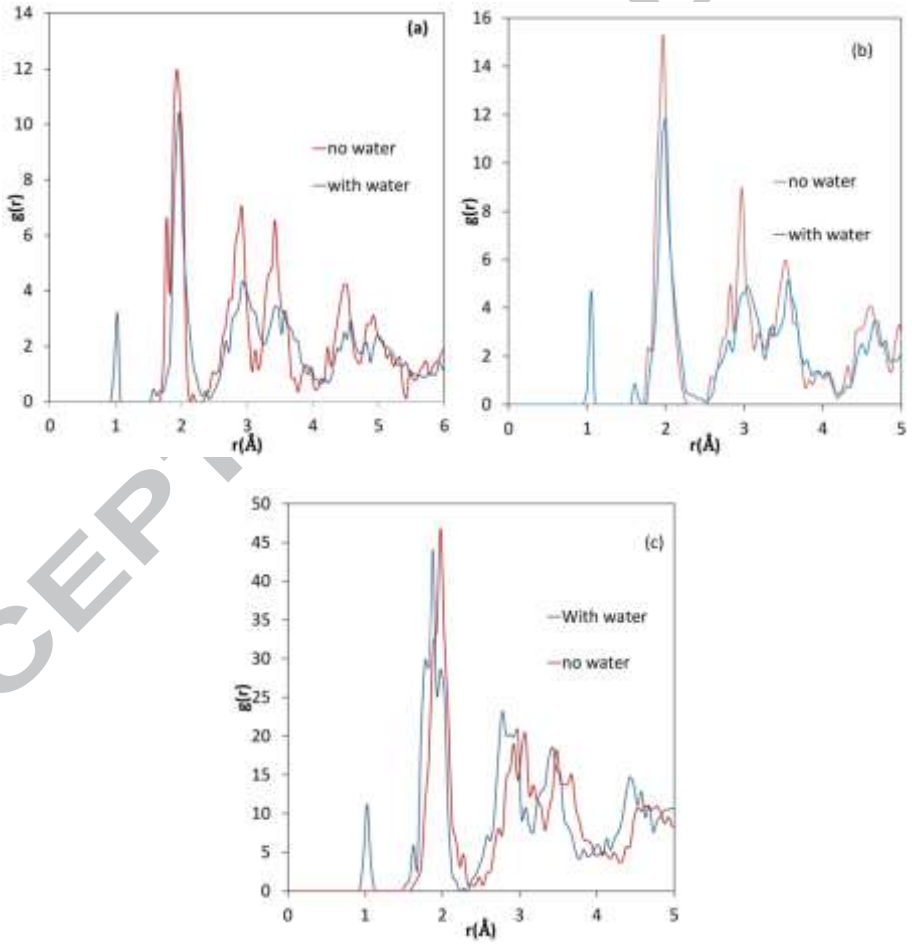

Figure 2.

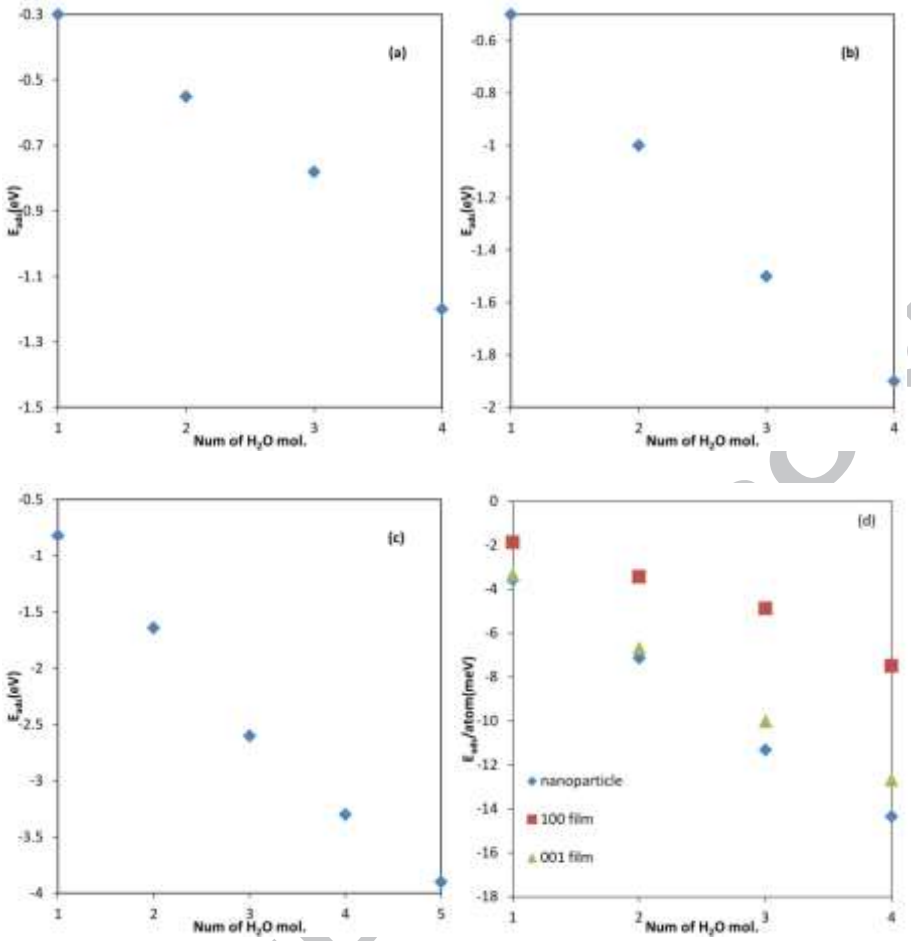

Figure 3.

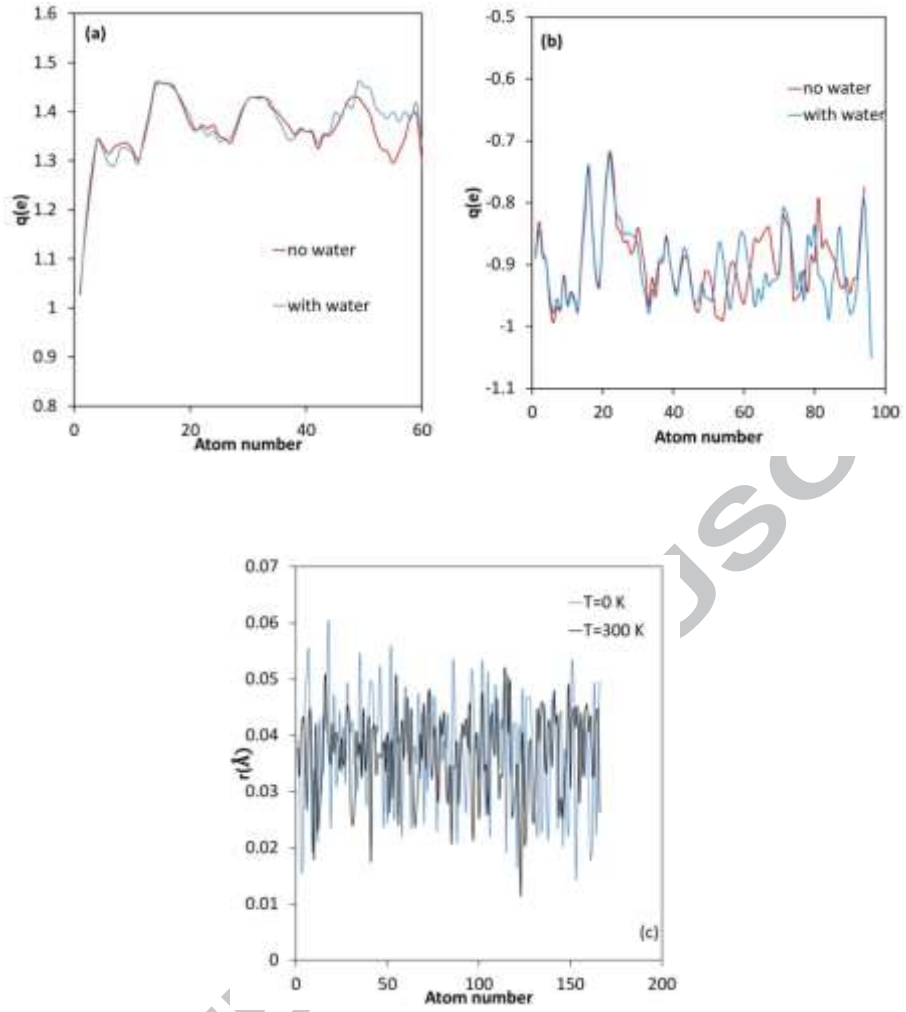

Figure 4.

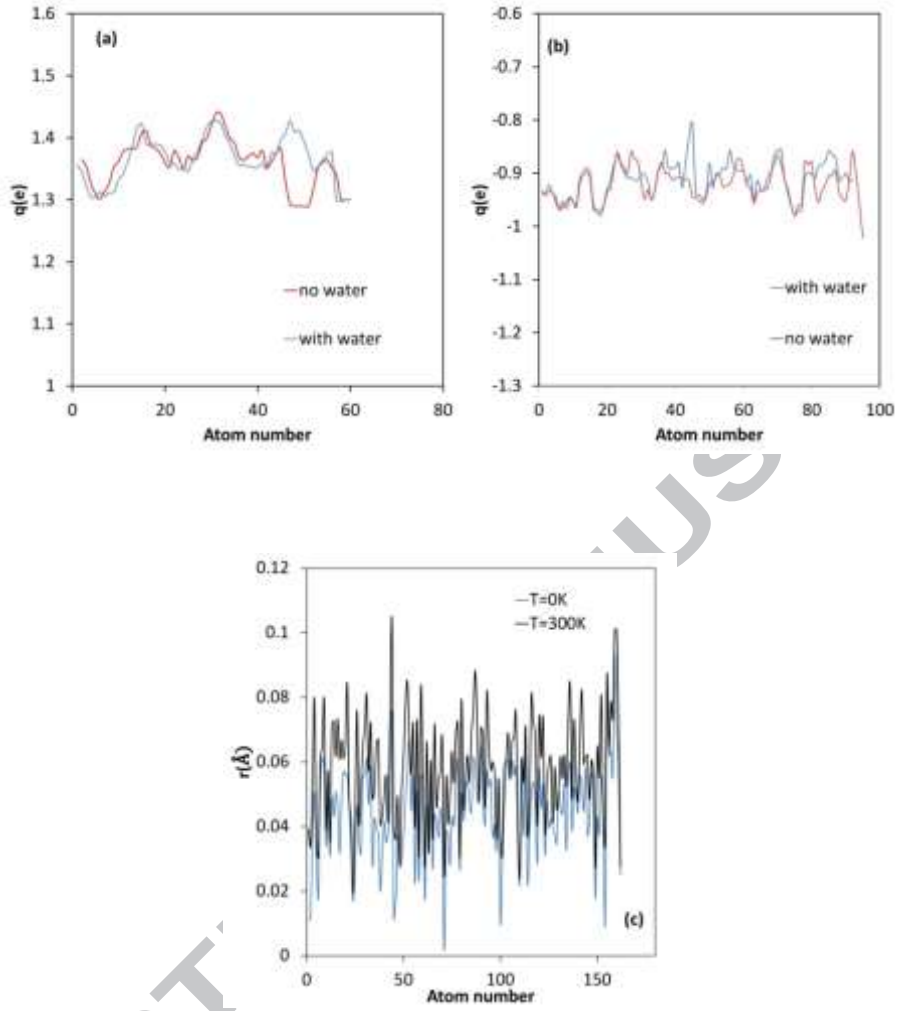

Figure 5.

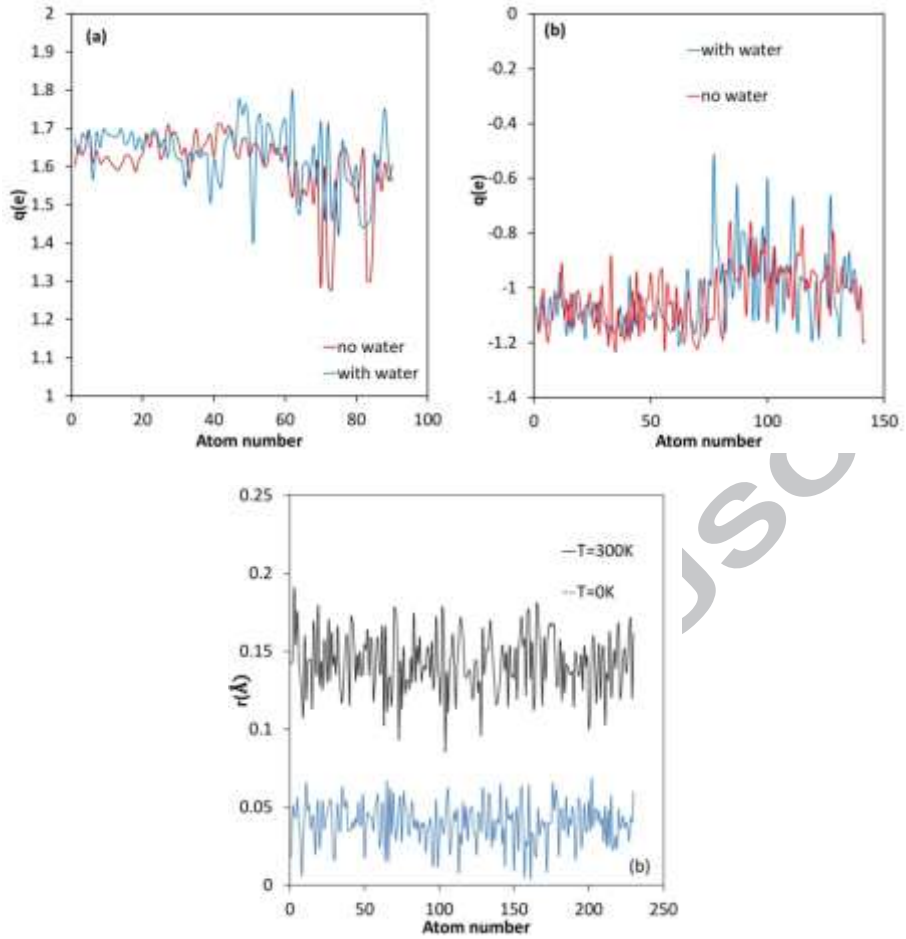

Figure 6.

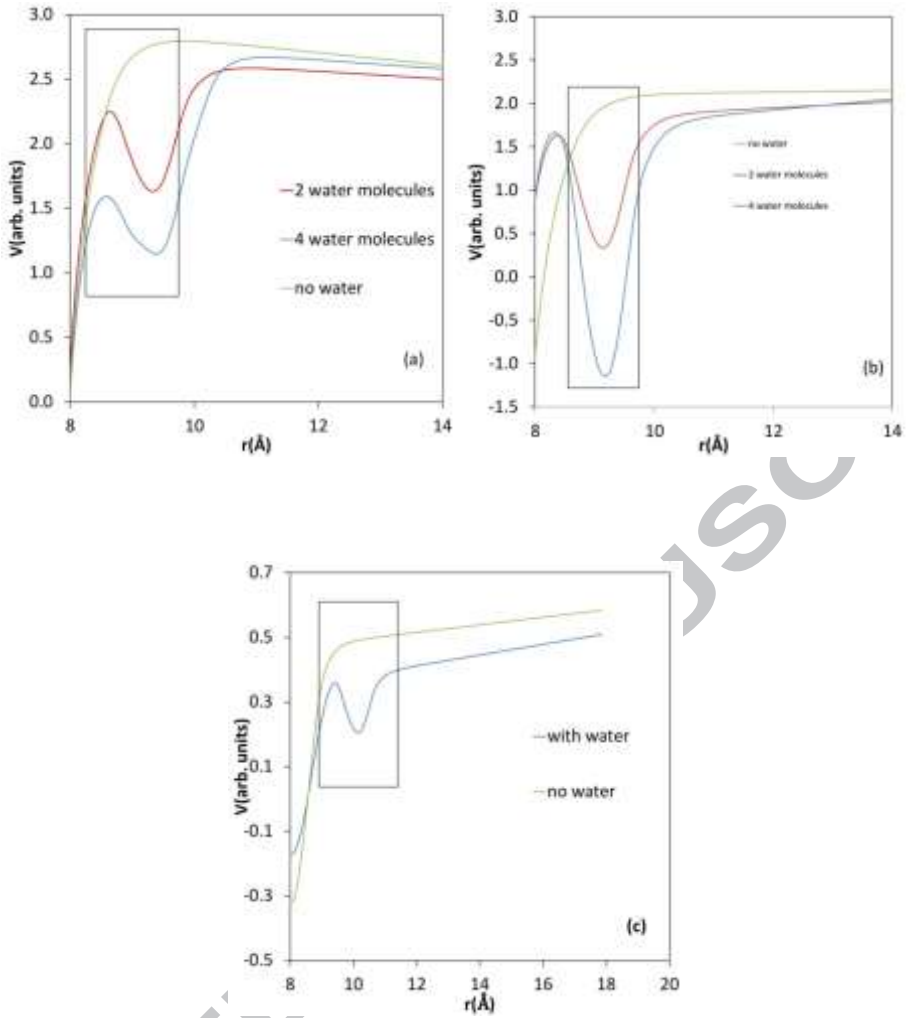

Figure 7.

Tables

a/a	Charge no water	Charge with water
Fe	1.09	1.19
Fe	1.38	1.39
Fe	1.31	1.34
O_w	-1.31	-1.19
O_w	-1.31	-1.21
O_w	-1.31	-1.22
O_w	-1.31	-1.20
H_w	0.65	0.62
H_w	0.65	0.60

Table 1

a/a	Charge no water	Charge with water
Fe	1.34	1.37
Fe	1.34	1.38
Fe	1.32	1.41
O_w	-1.31	-1.17
O_w	-1.31	-1.17
O_w	-1.31	-1.18
O_w	-1.31	-1.16
H_w	0.65	0.61
H_w	0.65	0.62

Table 2

Table 3

a/a	Charge no water	Charge with water
Fe	1.20	1.25
Fe	1.12	1.21
Fe	1.24	1.40
O_w	-1.31	-1.20
O_w	-1.31	-1.24
O_w	-1.31	-1.21
O_w	-1.31	-1.16
H_w	0.65	0.61
H_w	0.65	0.62

Table 4

Structure	M without water(μ_B/Fe atom)	M with water (μ_B/Fe atom)
100 film	1.22	1.19
001 film	1.77	1.65
spherical nanoparticle	1.85	1.71

Maghemite nanostructures as new materials for thermoelectric applications.

DFT molecular dynamics calculations on film and nanoparticle structures to study:

a)the adsorption energy of the water molecules attached on the surface of the maghemite structures.

b)the charge distribution before and after the addition of water

c)the electric field on interfaces between maghemite and water molecules structures.

d)Calculation of the zeta potential for the estimation of the strength of interaction between the nanostructures with the environment.